Whittaker function approach to determine the impurity energy levels of coated quantum dots

Ming-Chieh Lin and Der-San Chuu

Articles you may be interested in

Effects of electric field and shape on the ground state energy of an exciton bound to an ionized donor impurity in ellipsoidal quantum dots
J. Appl. Phys. **114**, 194301 (2013); 10.1063/1.4831664

The inter-sublevel optical properties of a spherical quantum dot-quantum well with and without a donor impurity
J. Appl. Phys. **112**, 053717 (2012); 10.1063/1.4751483

The electronic properties of a core/shell/well/shell spherical quantum dot with and without a hydrogenic impurity
J. Appl. Phys. **111**, 083702 (2012); 10.1063/1.3702874

Binding energy of a hydrogenic donor impurity in a rectangular parallelepiped-shaped quantum dot: Quantum confinement and Stark effects
J. Appl. Phys. **101**, 093716 (2007); 10.1063/1.2734097

Binding energy of impurity states in spherical quantum dots with parabolic confinement
J. Appl. Phys. **83**, 3089 (1998); 10.1063/1.367065

Whittaker function approach to determine the impurity energy levels of coated quantum dots

Ming-Chieh Lin and Der-San Chuu[a]

Department of Electrophysics, National Chiao Tung University, Hsinchu, Taiwan 30050, Republic of China

The electronic structure of a hydrogenic impurity atom located at the center of a multilayer coated quantum dot (CQD) is investigated. The electronic eigenstates of the CQD system are expressed in terms of the geometry and the material parameters by solving the Schrödinger equations analytically. Image potential effects are ignored and the effective mass approximation is employed. The ground state energy is found to be strongly influenced by the shell thickness and confined potential. In contrast to previous work, our eigenfunctions are expressed in terms of the Whittaker functions in any region, no matter where the energy levels are, i.e., whether they are higher or lower than the potential barriers. Our approach is simpler and has general significance, e.g., the bound state eigenenergies of any n-layered quantum dot can be easily determined by directly solving just "one" $(2n-2)$-rank secular determinant equation instead of solving 2^n equations. One can also easily and quickly determine whether a system has bound states by using the Whittaker function approach. © *2001 American Institute of Physics.* [DOI: 10.1063/1.1397282]

I. INTRODUCTION

In recent years, due to the advancement of modern crystal-growth techniques, it has been possible to fabricate various quasilow-dimensional structures of semiconductors such as quasitwo-dimensional quantum wells (QWs), quasione-dimensional quantum well wires (QWWs) and quasizero-dimensional quantum dots (QDs). These structures are obtained when the spatial dimensions of the conventional structures are reduced to those comparable to or less than the de Broglie wavelength of the carriers. For QDs, the ultimate goal is an artificial atom whose properties can be controlled well through the material parameters and geometry.[1] Recently, the electronic structures of the quantum dot, especially the donor states, acceptor states, and excitons, have received much attention. As a result of their possible applications in microelectronic devices, the quantum structures have been the subject of extensive theoretical and experimental research.

Much theoretical work has been devoted to the study of the properties of electronic states in various confining systems. Bastard[2] reported the first calculation for binding energies of hydrogenic impurities in QWs. In his calculation, the binding energy of a hydrogenic impurity was found to vary with the position of the impurity and with the thickness of the well. Brown and Spector[3] and Weber *et al.*[4] reported calculations of binding energies and density of impurity states in GaAs$-$(Ga,Al)As QWWs as a function of the radius of the structure. Zhu, Xiong and Gu[5] considered the hydrogenic donor states in a spherical quantum dot of GaAs$-$Al$_x$Ga$_{1-x}$As. They reported that the binding energy for the ground state of a donor at the center of a quantum dot is strongly dependent on the dimensionality and barrier height. In previous work, the impurity states in quantum dots

and quantum wires for the infinite potential confinement,[6] the Whittaker functions and Coulomb wave functions for the impurity eigenfunctions of the quantum dot were obtained for different energy ranges. The calculated result showed that the ground state energy of the impurity approaches the correct limit of the three-dimensional hydrogen atom as the radius of the quantum dot becomes very large.

Recently, it has proven possible to fabricate multilayer quantum dots which are composed of different semiconductor materials in each layer. In analogy to quantum well structures, they have been named quantum dot quantum wells,[7–9] or, simply, a coated quantum dots (CQDs). An extended theoretical approach for calculating the $1s-1s$ electronic transition in spherical layered semiconductor quantum dots was presented by Schooss *et al.*[10] Their calculations were carried out for the quantum dot quantum well CdS/HgS/CdS and compared to recently available experiment results. In their approach, a linear combination of the spherical Bessel and Neumann functions for the electron eigenfunctions of the CQD was assumed in regions where the energy level is lower than the potential barrier ($E<V$), and a linear combination of the two Hankel functions was proposed in regions where the energy level is higher than the potential barrier ($E>V$).

In the present study, we investigate the electronic structure of a hydrogenic impurity atom located at the center of a quasizero-dimensional CQD. Our model is constructed as a dot made of one kind of semiconductor material surrounded by a layer of another kind and then embedded into a different bulk material. It is obvious that the coated quantum dot will be equivalent to the simple quantum dot if the confinement potential in the shell is equal to that in the bulk (outside the shell). The geometrical shape of the coated quantum dot is chosen as spherical, because it is easier to solve. In the CQD system, we solve the Schrödinger equations analytically, and obtain the electronic eigenstates as functions of the geometry and the material parameters theoretically. Image potential ef-

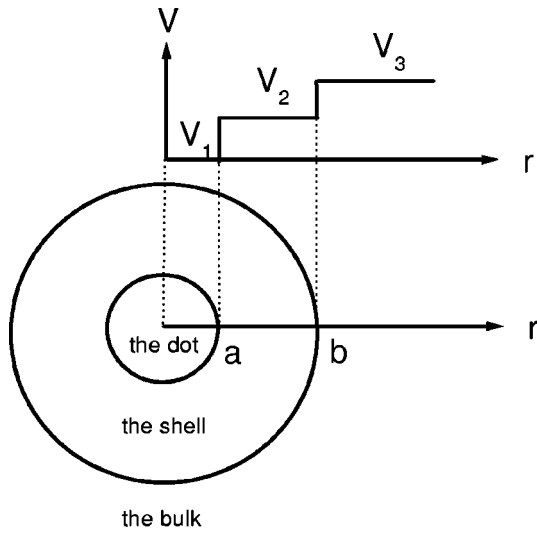[a]Corresponding author; electronic mail: dschuu@cc.nctu.edu.tw

FIG. 1. Schematic of the cross section and the confinement potential of the coated quantum dot.

fects in our system are ignored[11] and the effective mass approximation is employed although it is not always perfect.[12] In our treatment, the eigenfunctions are always expressed in terms of Whittaker functions only, no matter where the energy levels are, i.e., whether they are higher or lower than the potential barriers. After employing the boundary conditions, the eigenenergies are obtained by solving "one" four-rank secular determinant equation, although imaginary numbers might appear during the calculation. When we deal with bound states, the imaginary part of the energy E approaches zero automatically. The numerical result of the ground state energy is presented in the present work for illustration. We must emphasize here that our treatment is simpler than those of previous works in which it was assumed that a different form of eigenfunction exists in different energy regions. Conventionally, we must choose one of two wave functions corresponding to $E < V$ and $E > V$ in each layer, i.e., 2^n equations for a n-layered quantum dot.[3–5,10,13] On the other hand, by using the Whittaker function approach, one can study n-layered quantum dots by directly solving only "one" $(2n-2)$-rank secular determinant equation instead of 2^n equations.

II. FORMULATION

In this work, the system of a coated quantum dot with a hydrogenic impurity located at the center of the CQD is investigated. We deal with the bound state of the coated quantum dot which is like the quantum dot but with an additional layer embedded into a bulk material and each layer corresponds to one kind of material. The potential inside the dot is assumed to be zero ($V_1 = 0$), and inside the shell ($a \leqslant r \leqslant b$) it is V_2, while outside the shell ($r > b$) it is V_3. One should refer to Fig. 1 for a schematic view of the cross section of the coated quantum dot. The Hamiltonian of the system we considered can be written as

$$H = -\frac{\hbar^2}{2\mu}\nabla^2 - \frac{Ze^2}{\epsilon r} + V(r), \qquad (1)$$

where μ is the effective mass, ϵ is the dielectric constant, Z is the atomic number and

$$V(r) = \begin{cases} V_1 & \text{for } r \leqslant a, \\ V_2 & \text{for } a \leqslant r \leqslant b, \\ V_3 & \text{for } r \geqslant b. \end{cases} \qquad (2)$$

The Schrödinger equation can be expressed as

$$\left(-\frac{\hbar^2}{2\mu}\nabla^2 - \frac{Ze^2}{\epsilon r} + V(r)\right)\Psi(r,\theta,\varphi) = E\Psi(r,\theta,\varphi). \quad (3)$$

In spherical coordinates, the Schrödinger equation can be expressed as

$$-\frac{\hbar^2}{2\mu}\left[\frac{\partial^2}{\partial r^2} + \frac{2}{r}\frac{\partial}{\partial r} + \frac{1}{r^2\sin\theta}\frac{\partial}{\partial\theta}\left(\sin\theta\frac{\partial}{\partial\theta}\right)\right.$$
$$\left. + \frac{1}{r^2\sin^2\theta}\frac{\partial^2}{\partial\varphi^2}\right]\Psi(r,\theta,\varphi)$$
$$- \frac{Ze^2}{\epsilon r}\Psi(r,\theta,\varphi) + V(r)\Psi(r,\theta,\varphi) = E\Psi(r,\theta,\varphi), \qquad (4)$$

where $V(r)$ is defined in Eq. (2). We can solve Eq. (4) by separating the variables. Let $\Psi(r,\theta,\varphi) = R(r)\Theta(\theta)\Phi(\varphi)$, where $\Theta(\theta)$ is the associated Legendre polynomial and $\Phi(\varphi) = e^{im\varphi}$; m is an integer. The differential equation for the radial function $R(r)$ can be written as

$$-\frac{\hbar^2}{2\mu}\left(\frac{d^2}{dr^2} + \frac{2}{r}\frac{d}{dr} + \frac{L(L+1)}{r^2}\right)R(r) - \frac{Ze^2}{\epsilon r}R(r)$$
$$+ V(r)R(r) = ER(r), \qquad (5)$$

where L is 0 or a positive integer and $V(r)$ is defined in Eq. (2).

A. Inside the dot ($r < a$)

We use $R_1(r)$ to denote the wave function of the radial part in this region. Define

$$\alpha_1^2 = -\frac{8\mu_1(E-V_1)}{\hbar^2}; \quad \lambda_1 = \frac{2\mu_1 Ze^2}{\hbar^2\epsilon_1\alpha_1}; \qquad (6)$$

and let $\xi = \alpha_1 r$, then Eq. (5) can be expressed as

$$\frac{d^2 R_1(\xi)}{d\xi^2} + \frac{2}{\xi}\frac{dR_1(\xi)}{d\xi} + \left[-\frac{1}{4} + \frac{\lambda_1}{\xi} + \frac{\frac{1}{4}-(L+\frac{1}{2})^2}{\xi^2}\right]R_1(\xi)$$
$$= 0. \qquad (7)$$

To eliminate the term $dR_1(\xi)/d\xi$, we let $R_1(\xi) = \xi^{-1}\chi_1(\xi)$. Equation (7) then becomes

$$\frac{d^2\chi_1(\xi)}{d\xi^2} + \left[-\frac{1}{4} + \frac{\lambda_1}{\xi} + \frac{\frac{1}{4}-\left(L+\frac{1}{2}\right)^2}{\xi^2}\right]\chi_1(\xi) = 0, \qquad (8)$$

which is the Whittaker equation. The solutions of the above differential equation can be found in many mathematical handbooks. The following two solutions satisfy Eq. (8)

$$F_{\lambda_1,L}(\xi) = e^{-(\xi/2)}\xi^{L+1}F(L+1-\lambda_1, 2L+2, \xi), \qquad (9)$$

where

$$F(a,b,c)=1+\frac{a}{b}c+\frac{a(a+1)}{b(b+1)}\frac{c^2}{2!}+\cdots=\sum_{k=0}^{\infty}\frac{(a)_k}{(b)_k}\frac{c^k}{k!}.$$

The other solution is

$$G_{\lambda_1,L}(\xi)=e^{-(\xi/2)}\xi^{L+1}U(L+1-\lambda_1,2L+2,\xi),\qquad(10)$$

where

$$U(a,b,c)=\frac{(-1)^{2L+2}}{(2L+1)!\Gamma(a-b+1)}\left(\sum_{k=0}^{\infty}\frac{(a)_k}{(b)_k}\frac{c^k}{k!}\right.$$

$$\times[\ln c+\psi(a+k)-\psi(b+k)-\psi(k+1)]$$

$$+\frac{\Gamma(b-1)\Gamma(b)\Gamma(a-b+1)}{\Gamma(a)(-1)^{2L+2}}$$

$$\left.\times\sum_{r=0}^{b-2}\frac{(a-b+1)_r}{(2-b)_r}\frac{c^{r-2L-1}}{r!}\right);$$

$\Gamma(x)$ is the gamma function and $\psi(a)=d\ln\Gamma(a)/da$ is the digamma function. The $\ln\xi$ in Eq. (10) will cause the wave function to diverge at $r\sim0$. Therefore we must drop $G_{\lambda_1,L}(\xi)$, so that the wave function of the radial part in the core can be represented as

$$R_1(\alpha_1 r)=C_{11}e^{-(\alpha_1 r/2)}(\alpha_1 r)^L F(L+1-\lambda_1,2L+2,\alpha_1 r),$$
$$(11)$$

where C_{11} is the normalization constant.

B. Inside the shell ($a\leqslant r\leqslant b$)

We use $R_2(r)$ to denote the wave function of the radial part in this region. Define

$$\alpha_2^2=-\frac{8\mu_2(E-V_2)}{\hbar^2};\quad\lambda_2=\frac{2\mu_2 Ze^2}{\hbar^2\epsilon_2\alpha_2}.\qquad(12)$$

Likewise, we can write the wave function as

$$R_2(\alpha_2 r)=C_{21}e^{-(\alpha_2 r/2)}(\alpha_2 r)^L F(L+1-\lambda_2,2L+2,\alpha_2 r)$$

$$+C_{22}e^{-(\alpha_2 r/2)}(\alpha_2 r)^L U(L+1-\lambda_2,2L+2,\alpha_2 r),$$
$$(13)$$

where C_{21} and C_{22} are normalization constants.

C. Outside the shell ($r\geqslant b$)

We use $R_3(r)$ to denote the wave function of the radial part in this region. Define

$$\alpha_3^2=-\frac{8\mu_3(E-V_3)}{\hbar^2};\quad\lambda_3=\frac{2\mu_3 Ze^2}{\hbar^2\epsilon_3\alpha_3}.\qquad(14)$$

Likewise, we can write the wave function as

$$R_3(\alpha_3 r)=C_{31}e^{-(\alpha_3 r/2)}(\alpha_3 r)^L F(L+1-\lambda_3,2L+2,\alpha_3 r)$$

$$+C_{32}e^{-(\alpha_3 r/2)}(\alpha_3 r)^L U(L+1-\lambda_3,2L+2,\alpha_3 r),$$
$$(15)$$

where C_{31} and C_{32} are normalization constants, but the first term has to be dropped because it contains the $e^{-(\alpha_3 r/2)}F$ term which approaches $e^{\frac{\alpha_3 r}{2}}$ since $r\to\infty$ is divergent, so we must put $C_{31}=0$.

D. At the boundary ($r=a,r=b$)

Since the wave function and its derivative should be continuous at the boundary(s), the boundary conditions yield the following equations:

$$\begin{cases}R_1(\alpha_1 a)=R_2(\alpha_2 a),\\[4pt]\dfrac{R_1'(\alpha_1 a)}{\mu_1}=\dfrac{R_2'(\alpha_2 a)}{\mu_2},\\[4pt]R_2(\alpha_2 b)=R_3(\alpha_3 b),\\[4pt]\dfrac{R_2'(\alpha_2 b)}{\mu_2}=\dfrac{R_3'(\alpha_3 b)}{\mu_3}.\end{cases}\qquad(16)$$

The above equations become

$$\begin{vmatrix}-R_{11}&R_{21}&R_{22}&0\\[4pt]-\dfrac{R_{11}'}{\mu_1}&\dfrac{R_{21}'}{\mu_2}&\dfrac{R_{22}'}{\mu_2}&0\\[4pt]0&R_{21}&R_{22}&-R_{32}\\[4pt]0&\dfrac{R_{21}'}{\mu_2}&\dfrac{R_{22}'}{\mu_2}&-\dfrac{R_{32}'}{\mu_3}\end{vmatrix}\begin{pmatrix}C_{11}\\C_{21}\\C_{22}\\C_{32}\end{pmatrix}=0.\qquad(17)$$

For a nontrivial solution to exist, the determinant of the co-efficients must vanish, which implies

$$\left\{\left[\frac{\alpha_3\mu_2}{\alpha_2\mu_3}\left(-\frac{1}{2}+\frac{U_{3b}'}{U_{3b}}\right)+\frac{1}{2}\right]U_{2b}-U_{2b}'\right\}$$

$$\times\left\{F_{2a}'-\left[\frac{\alpha_1\mu_2}{\alpha_2\mu_1}\left(-\frac{1}{2}+\frac{F_{1a}'}{F_{1a}}\right)+\frac{1}{2}\right]F_{2a}\right\}$$

$$=\left\{\left[\frac{\alpha_1\mu_2}{\alpha_2\mu_1}\left(-\frac{1}{2}+\frac{F_{1a}'}{F_{1a}}\right)+\frac{1}{2}\right]U_{2a}-U_{2a}'\right\}$$

$$\times\left\{F_{2b}'-\left[\frac{\alpha_3\mu_2}{\alpha_2\mu_3}\left(-\frac{1}{2}+\frac{U_{3b}'}{U_{3b}}\right)+\frac{1}{2}\right]F_{2b}\right\},\qquad(18)$$

where

$$F_{1a}=F(L+1-\lambda_1,2L+2,\alpha_1 a);$$

$$U_{2a}=U(L+1-\lambda_2,2L+2,\alpha_2 a);$$

$$F_{2a}=F(L+1-\lambda_2,2L+2,\alpha_2 a);$$

$$U_{2b}=U(L+1-\lambda_2,2L+2,\alpha_2 b);$$

$$F_{2b}=F(L+1-\lambda_2,2L+2,\alpha_2 b);$$

$$U_{3b}=U(L+1-\lambda_3,2L+2,\alpha_3 b);$$

Eq. (18) is used to yield the eigenenergy E.

III. RESULTS AND DISCUSSION

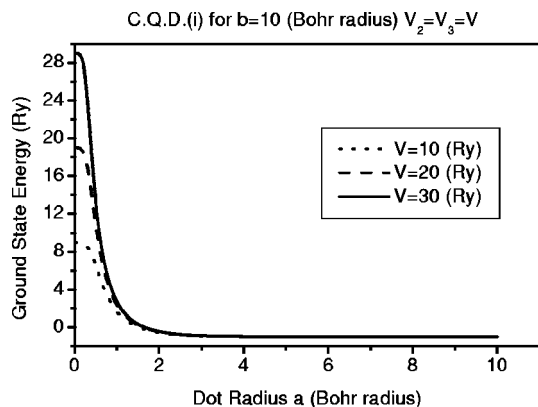We have calculated the ground state energy of an electron confined in a coated quantum dot with a hydrogenic

FIG. 2. Ground state energy of the electron bound inside the coated quantum dot with an impurity located at the center for $V = (10,20,30)$ Ry and $b = 10\, a_0^*$ (the effective Bohr radius).

FIG. 4. Ground state energy vs V_2 of the electron inside the coated quantum dot with an impurity located at the center for $V_3 = 10$ Ry, $a = 1 a_0^*$ and $b = (1.1,1.2)a_0^*$, i.e., the shell thickness is equal to 0.1 and $0.2a_0^*$, respectively.

impurity located at the center. The confinement potential is zero ($V_1 = 0$) inside the core, V_2 in the shell, and V_3 outside the shell. In this work, the length and the energy are expressed in terms of the effective Bohr radius $a_0^* = \epsilon \hbar^2 / \mu Z e^2$ and the effective Rydberg $Ry = Z e^2 / 2 \epsilon a_0^*$. In order to realize how the geometry and confined potential affect the eigenenergy, we assume the dielectric constant corresponding to each layer is approximately equal to one another, and so is the effective mass, i.e., $\epsilon_1 \sim \epsilon_2 \sim \epsilon_3$ and $\mu_1 \sim \mu_2 \sim \mu_3$. When the confinement potential V_2 in the shell is equal to V_3 outside the shell ($V_2 = V_3 = V$), our system is reduced to the case of the quantum dot again. For the case of the quantum dot, as the dot radius approaches ∞, the impurity located at the center of the coated quantum dot behaves like a free hydrogenic atom and the ground state energy approaches -1 Ry. When the dot radius decreases, the ground state energy of the electron gradually increases. As the dot radius is reduced more and more, the confinement effect pushes the ground state energy of the electron to become larger and larger. Finally, the electron cannot be bound inside the dot and thus becomes a free hydrogenic atom again. This makes the ground state energy of the electron approach (V

-1) Ry. Figure 2 shows our calculated ground state energy of the electron inside the coated quantum dot with an impurity for $V = (10,20,$ and $30)$ Ry and $b = 10 a_0^*$. From Fig. 2, one can see that the ground state energy approaches the correct limits. Furthermore, steeper curves are obtained for higher confinement potential. The ground state energy is equal to zero at different dot radii when the potential barrier is different. Figure 3 shows that the ground state energy is equal to zero at larger dot radius (a^*) if the potential barrier is higher. We can compare these results with our previous work.[6] In the previous work, the ground state energy became negative when the dot radius was larger than $1.833 a_0^*$ for an infinite potential barrier. In this work, the ground state energy equals zero at dot radius of $1.833\,01 a_0^*$ when the potential barrier V is equal to $10\,000$ Ry. For $V = 10$ Ry, $a^* = 1.609\,55 a_0^*$.

Now, let us consider the case of $V_2 \neq V_3$. Figure 4 presents our calculated ground state energy versus V_2 of the electron inside the coated quantum dot with an impurity located at the center for $V_3 = 10$ Ry, $a = 1 a_0^*$ and $b = (1.1,1.2)a_0^*$, i.e., the shell thickness is equal to 0.1 and 0.2 a_0^*, respectively. One can see from Fig. 4 that the ground
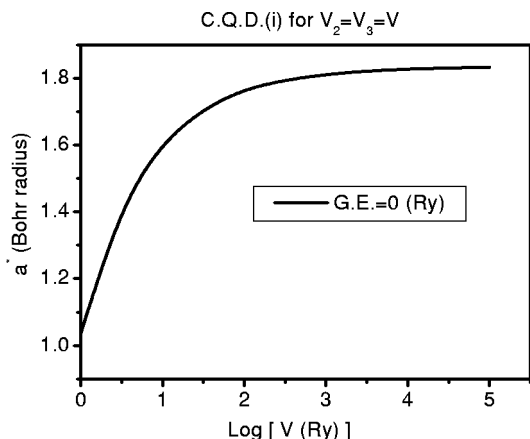

FIG. 3. Ground state energy of the electron bound inside the coated quantum dot with an impurity located at the center equal to zero at different dot radii when the potential barrier is different. The ground state energy equals zero at larger dot radius (a^*) if the potential barrier is higher.
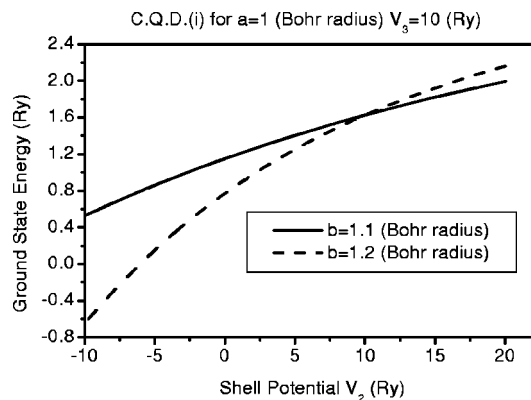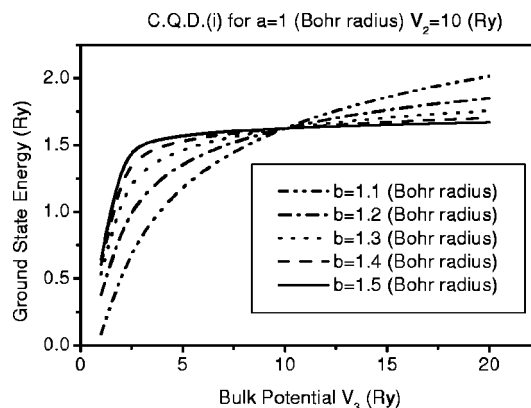

FIG. 5. Ground state energy vs V_3 of the electron inside the coated quantum dot with an impurity located at the center for $V_2 = 10$ Ry, $a = 1 a_0^*$ and $b = (1.1,1.2,1.3,1.4,1.5)a_0^*$, i.e., the shell thickness is equal to 0.1,0.2,0.3,0.4 and $0.5a_0^*$, respectively.
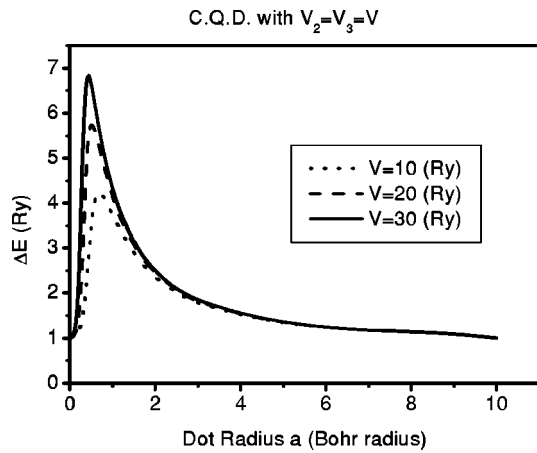
FIG. 6. Energy difference ΔE with $V_2=V_3=V=(10,20,30)$ Ry and $b=10\,a_0^*$.

FIG. 8. Energy difference ΔE for $b=(1.1,1.2)a_0^*$, i.e., the shell thickness is equal to 0.1 and $0.2a_0^*$, respectively.

state energy increases when the shell potential V_2 increases ($V_2 \geqslant V_3$). When the shell potential decreases ($V_2 \leqslant V_3$), the ground state energy also decreases. Furthermore, steeper curves are obtained for thicker shells. Figure 5 presents our calculated ground state energy versus V_3 of the electron inside the coated quantum dot with an impurity located at the center for $V_2=10$ Ry, $a=1$ a_0^* and $b=(1.1,1.2,1.3, 1.4,1.5)a_0^*$, i.e., the shell thickness is equal to 0.1,0.2,0.3,0.4 and 0.5 a_0^*, respectively. One can see from Fig. 5 that the ground state energy increases when the bulk potential increases for $V_3 \geqslant V_2$. When the bulk potential decreases, the ground state energy also decreases for $V_3 \leqslant V_2$. Furthermore, larger slope curves are obtained for thinner shells. Figures 4 and 5 also show that the ground state energy is strongly influenced by the shell thickness. In the case of $V_3 \leqslant V_2$, the eigenvalues are found to become complex numbers when the bulk potential V_3 is lowered enough. This implies that there are no bound states in this situation. Thus, we can easily and quickly determine whether a system has bound states by the Whittaker function approach.

The energy difference ΔE due to Coulomb interaction is defined as the ground state energy of an electron alone inside the coated quantum dot minus the ground state energy of an electron inside the coated quantum dot with an impurity. And
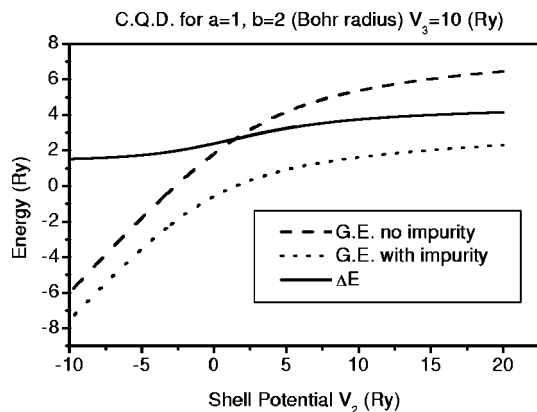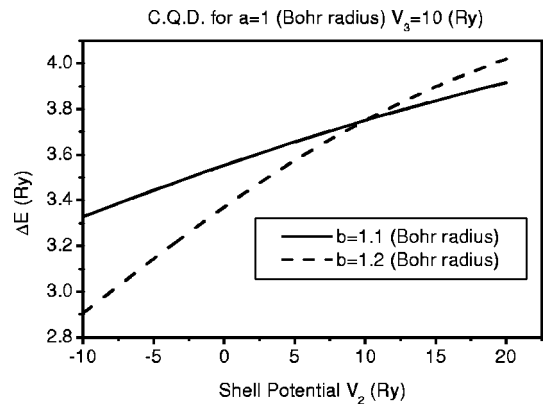
the ground state energy of an electron alone inside the coated quantum dot can be easily obtained by putting the parameter λ equal to zero. Figure 6 shows the energy difference ΔE with $V_2=V_3=V=(10,20,$ and $30)$ Ry and $b=10a_0^*$. From Fig. 6, one can see that the energy difference ΔE approaches the correct limits as the dot radius approaches ∞ or zero. In this case, the impurity located at the center of the coated quantum dot behaves like a free hydrogenic atom and the energy difference ΔE approaches 1 Ry, the binding energy of a free hydrogenic atom. Furthermore, one can see larger ΔE for steeper curves with higher confinement potential. The peak occurs at smaller dot radius for higher potential barriers.

Still, for the case of $V_2 \neq V_3$, Fig. 7 presents our calculated ΔE for $V_3=10$ Ry, $a=1a_0^*$ and $b=2$ a_0^*, i.e., the shell thickness is equal to $1a_0^*$. Figure 8 presents a similar situation for $b=(1.1,1.2)a_0^*$, i.e., the shell thickness is equal to 0.1 and $0.2a_0^*$, respectively. One can see from Figs. 7 and 8 that the energy difference ΔE increases when the shell potential V_2 increases ($V_2 \geqslant V_3$). When the shell potential decreases ($V_2 \leqslant V_3$), the energy difference ΔE also decreases. Furthermore, one can see steeper curves can be obtained for thicker shells. Figure 9 presents the energy difference ΔE vs V_3 for $V_2=10$ Ry, $a=1$ a_0^* and b

FIG. 7. Energy difference ΔE for $V_3=10$ Ry, $a=1a_0^*$ and $b=2a_0^*$, i.e., the shell thickness is equal to $1a_0^*$.
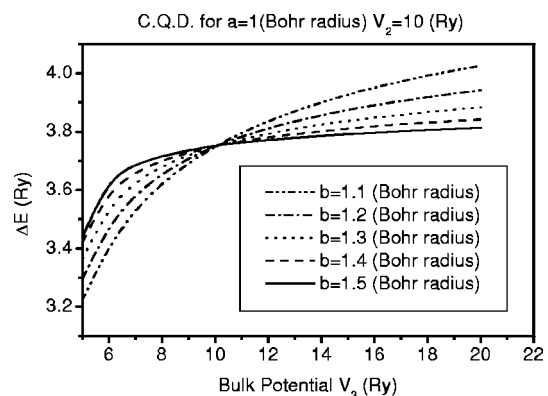

FIG. 9. Energy difference ΔE vs V_3 of the impurity located at the center of the coated quantum dot for $V_2=10$ Ry, $a=1a_0^*$ and $b=(1.1,1.2,1.3,1.4,1.5)a_0^*$, i.e., the shell thickness is equal to 0.1,0.2,0.3,0.4 and $0.5a_0^*$, respectively.

$=(1.1, 1.2, 1.3, 1.4, 1.5)a_0^*$, i.e., the shell thickness is equal to $0.1, 0.2, 0.3, 0.4$ and $0.5a_0^*$, respectively. One can see from Fig. 9 that the energy difference ΔE increases when the bulk potential V_3 increases $(V_3 \geqslant V_2)$. When the bulk potential decreases $(V_3 \leqslant V_2)$, the energy difference ΔE also decreases. One can also see steeper curves for thinner shells. So, the energy difference ΔE is strongly influenced by the shell thickness.

IV. CONCLUSION

In this study, we have investigated the electronic structures in a quasilow dimensional multilayer quantum system, the coated quantum dot. In the CQD system, we can solve the Schrödinger equations for a hydrogenic impurity analytically, and obtain the electronic eigenstates as functions of the geometry and the material parameters theoretically via the Whittaker function approach. All the eigenfunctions can be expressed in terms of Whittaker functions, and it does not matter whether the energy levels are higher or lower than the potential barriers although there are imaginary numbers in the latter case. For numerical calculations, we have only calculated the ground state energy for illustration purposes. It is shown that the ground state energy of the coated quantum dot is strongly influenced by the shell thickness and confined potential. In the case of $V_3 \leqslant V_2$, the eigenvalues become complex numbers when the bulk potential V_3 is lowered enough. This implies that there are no bound states in this situation. We can easily and quickly determine whether a system has bound states by the Whittaker function approach. We must emphasize again here that the Whittaker function method is a simpler approach with which to deal with multilayer quantum dots and it has general significance. One can study electronic structures of n-layered quantum dots by directly solving just "one" $(2n-2)$-rank secular determinant equation instead of by solving 2^n equations.

V. ACKNOWLEDGEMENT

[1] Z. Xiao, J. Zhu, and F. He, J. Appl. Phys. **79**, 12 (1996).

[2] G. Bastard, Phys. Rev. B **24**, 4714 (1981).

[3] J. Brown and H. N. Spector, J. Appl. Phys. **59**, 1179 (1986).

[4] G. Weber, P. A. Schulz, and L. E. Oliveira, Phys. Rev. B **38**, 2179 (1988); Mater. Sci. Forum **38–41**, 1415 (1989).

[5] J. L. Zhu, J. J. Xiong, and B. L. Gu, Phys. Rev. B **41**, 6001 (1990).

[6] D. S. Chuu, C. M. Hsiao, and W. N. Mei, Phys. Rev. B **46**, 3898 (1992).

[7] A. Eychmuller, A. Mews, H. Weller, Chem. Phys. Lett. **208**, 59 (1993).

[8] A. Eychmuller, T. Vossmeyer, A. Mews, and H. Weller, J. Lumin. **58**, 223 (1994).

[9] A. Mews, A. Eychmuller, M. Giersig, D. Schooss, and H. Weller, J. Phys. Chem. **98**, 934 (1994).

[10] D. Schooss, A. Mews, A. Eychmuller, and H. Weller, Phys. Rev. B **49**, 17 072 (1994).

[11] F. Stern and S. Das Sarma, Phys. Rev. B **30**, 840 (1984).

[12] S. V. Nair, L. M. Ramaniah, and K. C. Rustagi, Phys. Rev. B **45**, 5969 (1992).

[13] C. C. Yang, L. C. Liu, and S. H. Chang, Phys. Rev. B **58**, 1954 (1998).